Soft Magnetic Properties of Carbide-Dispersed Nanocrystalline Films with High Thermal Stability

N. Hasegawa, M. Saito, N. Kataoka, and H. Fujimori

Nanocrystalline Fe-M-C, Co-M-C, and Ni-M-C (M = group IVa-VIa metals) films in which extremely fine M-carbide particles are dispersed were prepared by annealing sputter-deposited amorphous alloy films. Of these films, the Fe-M-C and Co-M-C films exhibited good soft magnetic properties. These soft magnetic properties were maintained after annealing at elevated temperatures, because carbide particles dispersed in the films considerably retard the grain growth of Fe-rich or Co-rich nanocrystallites. Films containing Ta or Hf exhibit particularly high thermal stability (around 1000 K). On the other hand, Zr and Hf are suitable for obtaining high saturation magnetization, I_s, because the amount of these elements needed for amorphization is less than other M elements. The highest I_s of films containing Zr or Hf was 1.7 T for Fe-M-C and 1.6 T for Co-M-C films. Because the magnetostriction of Fe-M-C films is dominated primarily by the C concentration dissolved into Fe, zero-magnetostrictive films can easily be attained by controlling the C to M ratio or annealing conditions. In addition to the good performance of Fe-Hf-C films, a higher I_s value of 2.0 T was achieved by multilayering the Fe-Hf-C with Fe, and improved frequency characteristics of permeability as well as higher thermal stability by about 100 K was achieved by Si additions without sacrificing other properties. These carbide-dispersed nanocrystalline films are suitable for use in high-density magnetic recording heads fabricated by glass bonding processes.

Keywords
carbide dispersions, nanocrystalline films, soft magnetics

1. Introduction

RECENTLY, nanocrystalline soft magnetic thin films have been studied intensively because of their potential use in high-density recording heads and other applications. Although Fe- or Co-rich crystalline phases have higher saturation magnetization than that of conventional soft magnets like Fe-Si-Al, Ni-Fe alloys, or Co-base amorphous alloys, it was difficult to obtain soft magnetic properties because of their large magnetocrystalline anisotropy. Recently, however, there have been a number of reports that Fe-rich[1-6] and Co-rich[7] crystalline films become soft magnetic when the grain size is refined to a nanoscale order. An explanation of soft magnetism in these materials is based on the ripple theory[8,9] or the random anisotropy model.[10] The point of these explanations is that the magnetocrystalline anisotropy is averaged out through exchange and/or dipole-dipole interactions between nanocrystallites.

From a practical point of view, head core materials are required to have high thermal stability of their soft magnetic properties where glass bonding or other high-temperature processes are applied in head manufacture (e.g., metal-in-gap type heads). Despite the good performance in permeability and saturation magnetization, nanocrystalline materials generally are susceptible to grain growth when annealed at elevated temperatures, often resulting in deterioration of soft magnetic properties. To overcome this problem, the authors developed thermally stable nanocrystalline Fe-M-C[11,12] and Co-M-C[13] (M = group IVa-VIa metals) films, in which extremely fine M-carbide particles are dispersed. These films were prepared by nanocrystallization of sputter-deposited amorphous films and have good magnetic properties. The present article reviews their microstructure and magnetic properties, as well as further improvement in their performance by multilayering or Si addition within the framework of the carbide-dispersed nanocrystalline concept.

N. Hasegawa and **M. Saito**, Niigata Division Alps Electric Co., Ltd., Higashi-Takami, Nagaoka, Japan; **N. Kataoka** and **H. Fujimori**, Institute for Materials Research, Tohoku University, Sendai, Japan; **N. Kataoka**, present address Department of Materials Science, Tohoku University.

2. Experimental Procedure

Samples were deposited on partially crystallized glass substrates using an rf diode sputtering apparatus. Composite targets consisting of the pellets of the element M (Zr, Hf, Nb, Ta, etc.) placed on Fe, Co, or Ni targets were reactively sputter-deposited in an Ar + CH_4 atmosphere. Alternatively, films were prepared by conventional Ar ion sputtering using composite targets to which pellets of graphite and the element M were attached. The authors previously confirmed that there was no significant difference in the properties of the films prepared by these two methods.[11] For preparing Fe/Fe-Hf-C multilayers, a multisource type of rf sputtering apparatus with the graphite composite target and pure Fe target was used. During deposition, the rf power input was 2.4×10^4 W/m^2 and the total pressure was 0.67 Pa; the substrate holder was water cooled.

The film composition was analyzed by the combustion method for C content and electron probe microanalyzer (EPMA) for other elements. The saturation magnetization, I_s, the relative permeability, μ, and the coercivity, Hc, were measured using a vibrating sample magnetometer (VSM), the figure-eight coil method, and a dc B-H loop tracer, respectively. The optical cantilever method was used to measure magnetostriction, λs. Film structures were investigated by X-ray diffractometry and by transmission electron microscopy (TEM).

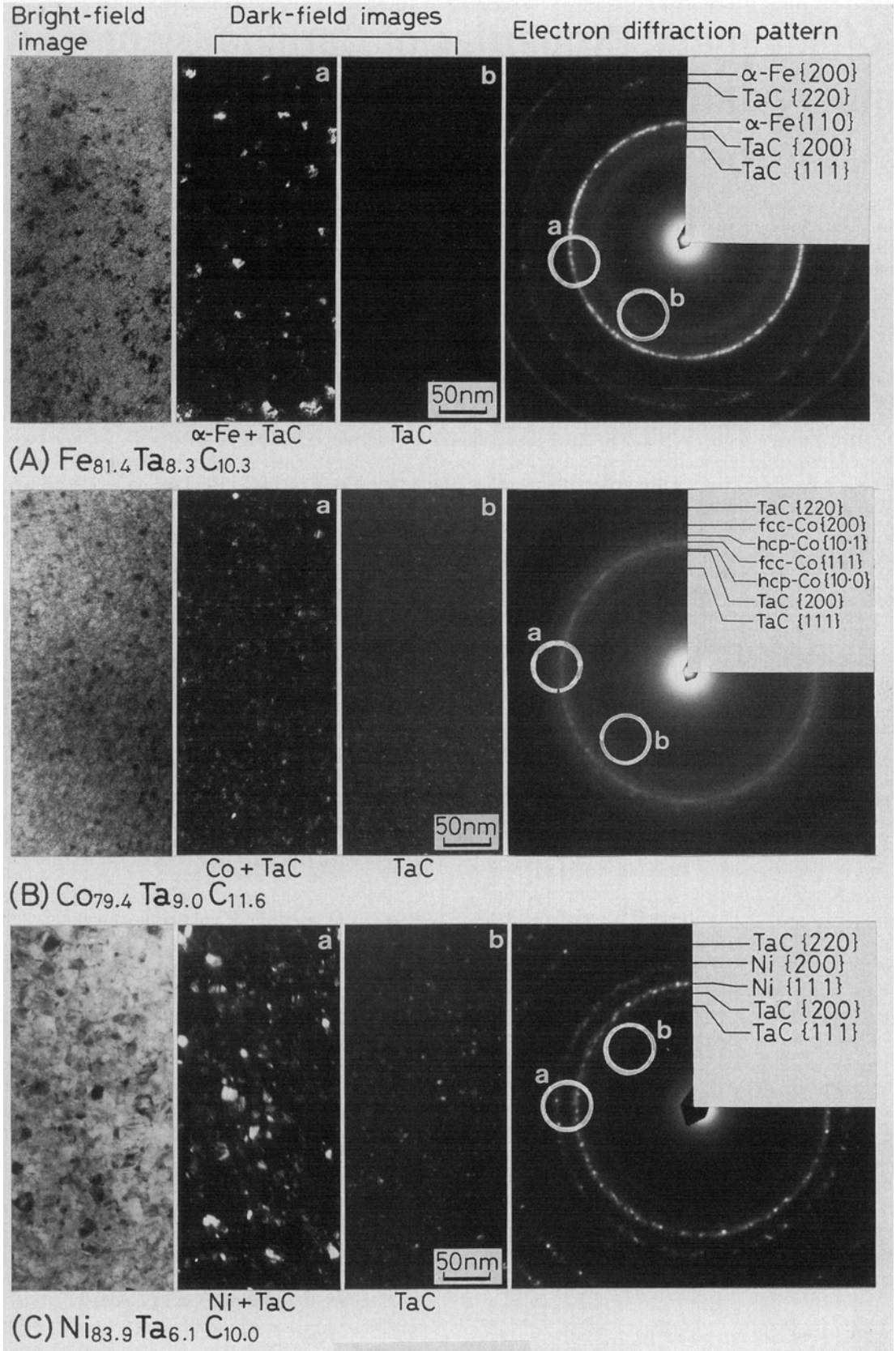

Fig. 1 TEM images and electron diffraction patterns of $Fe_{81.4}Ta_{8.3}C_{10.3}$ (a), $Co_{79.4}Ta_{9.0}C_{11.6}$ (b), and $Ni_{83.9}Ta_{6.1}C_{10.0}$ (c) films crystallized from an amorphous state by annealing at 823 K for 1.2 ks. The dark-field images (a and b) were taken with an objective aperture indicated with the circles in the diffraction patterns.

Samples for use in TEM observations in the plane of the film were prepared by peeling the films (5 μm thick) from the substrate and ion milling both sides of the films. Samples for cross-sectional TEM observations were prepared by polishing and ion milling.

3. Results and Discussion

3.1 *Microstructure of Films Crystallized from an Amorphous State*

In Fig. 1, TEM images and electron diffraction patterns of $Fe_{81.4}Ta_{8.3}C_{10.3}$, $Co_{79.4}Ta_{9.0}C_{11.6}$, and $Ni_{83.9}Ta_{6.1}C_{10.0}$ alloy films annealed at 823 K for 1.2 ks are shown. They were amorphous in an as-deposited state and crystallized into a nanocrystalline state by annealing. In each film, diffuse diffraction rings of TaC (NaCl-type structure) are observed. Dark-field images (Fig. 1B) taken from {111} reflection of TaC shows that extremely fine (approximately 1 to 4 nm) TaC grains are dispersed uniformly throughout each film. The main phase is bcc Fe for the Fe-Ta-C film (Fig. 1A), mixture of cph Co and fcc Co for the Co-Ta-C film (Fig. 1B), and fcc Ni for the Ni-Ta-C film (Fig. 1C). Their lattice spacings measured by X-ray diffractometry agree with that of the pure elements, except for bcc Fe. The lattice spacing of bcc Fe in the Fe-Ta-C films was larger than that of pure Fe by 0.5%. In Fig. 1, dark-field images (Fig. 1A) taken from reflections of both main phase (Fe, Co, or Ni) and TaC are also shown. As can be seen in these dark-field images, the Co grain in the Co-Ta-C film is the smallest (5 to 6 nm) and the Ni grain in the Ni-Ta-C films is the largest (10 to 30 nm) of the three. The Fe grain in the Fe-Ta-C film is 6 to 10 nm. By high-resolution TEM (HRTEM) observation of the Fe-Ta-C film,[14] most of the fine TaC grains were found to be located at the grain boundaries (mostly at triple junctions) of Fe grains, as schematically shown in Fig. 2. Because the nonmagnetic TaC grains are much smaller than the Fe grains, adjacent Fe grains are in contact through wide segments of grain boundaries. This contact between ferromagnetic grains enables exchange interaction, which makes the magnetization of each ferromagnetic grain nearly parallel, thus resulting in an averaging out of magnetocrystalline anisotropy. In general, nonmagnetic inclusions are thought to be harmful to soft magnetic properties. In these films, however, the nonmagnetic TaC particles do not act as wall pinning sites because they are two orders of magnitudes smaller than the wall thickness.

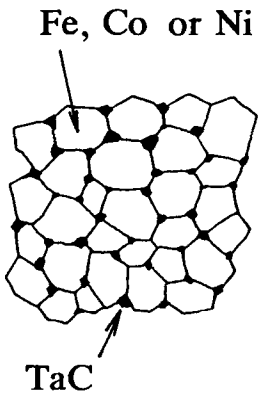

Fig. 2 Schematic of the microstructure of carbide-dispersed nanocrystalline films.

When Ta is replaced by other carbide-forming elements (Ti, Zr, Hf, V, Nb, etc.), a similar carbide-dispersed nanocrystalline structure is obtained.[11-13] The pseudobinary and pseudoternary (Fe,Co,Ni)-Ta-C alloy films in which Fe, Co, and Ni are combined also crystallize into nanocrystals from the amorphous state and also exhibit good soft magnetic properties over wide Fe:Co:Ni composition ranges after crystallization.[15]

3.2 *Nanocrystallization Behavior*

Fe-Cu-Nb-Si-B alloy[4] is a well-known nanocrystalline material that is also crystallized from an amorphous state. According to Ref 16 and 17, the mechanism of the formation of the nanocrystalline structure of this alloy involves Cu, which plays an important role for inducing compositional inhomogeneity in the amorphous phase at an early annealing stage. Such inhomogeneity causes increased density of the nucleation sites for crystallization. However, the present Fe-M-C or Co-M-C alloy films form nanocrystallites without an addition of nucleation-enhancing elements such as Cu. The mechanism of nanocrystallization was first thought to be such that the compositional inhomogeneity was induced in the early stage of annealing by the strong affinity between M and C.[18] Recently, however, atom probe field ion microscope (APFIM) analysis of the Fe-Ta-C films[19] revealed that concentration fluctuations of C on a nanometer scale develops independently of fluctuations in Ta in the early annealing stage. There is a possibility that this concentration fluctuation of C is caused by spinodal decomposition similar to that observed in the early stage of tempering of Fe-C-Ni martensites.[20] Nucleation of αFe may occur at the C-depleted region. Because αFe has only a few atomic percent of solubility with Ta, Ta would diffuse out of the crystallized regions into the amorphous phase, where the C concentration becomes higher. Then the TaC forms by nucleation from the C- and Ta-enriched amorphous region. The TaC may precipitate immediately after the precipitation of αFe, because only one exothermic peak is observed in the differential scanning calorimetry (DSC) curve.[18] Because the precipitated TaC has a high melting point and is extremely stable, it can pin the grain boundaries and works to retard grain growth during further heat treatment.

According to the above-mentioned mechanism for nanocrystallization of Fe-M-C films, the conditions required for element M for nanocrystallization are as follows: (1) solubility in αFe must be low, (2) carbide forming tendency must be high, and (3) formed carbide must be stable (high melting temperature). The elements that sufficiently fulfill these requirements are Zr, Hf, Nb, and Ta among group IVa-VIa elements. Actually, the Fe-M-C films containing these elements exhibit particularly fine grain structure after crystallization and improved soft magnetic properties than the films containing other group IVa-Va elements, as shown in Table 1 in which the typical magnetic properties of Fe-M-C (M = group IVa, Va) are summarized. This fact would support the validity of the assumed mechanism for nanocrystallization.

In Fig. 3, annealing temperature dependence of saturation magnetization, I_s, and resistivity, ρ, of some Fe-M-C films at room temperature is shown. The holding time at each annealing temperature was 1.2 ks. In an as-deposited state, I_s is low because M and C reduce the magnetic moment and the Curie temperature of Fe in the amorphous state. However, I_s rapidly rises by annealing at around 700 K and reaches a maximum at 1.7 T. This rapid rise in I_s is due to the crystallization because ρ falls sharply just around this temperature. This phenomenon is due to the phase separation of M and C from the αFe phase on crystallization.

Because the Curie temperature of the amorphous phase is much lower than that of the αFe crystallite, the amorphous phase is almost nonmagnetic at the temperatures where crystallization occurs.[14] Therefore, I_s at high temperature is proportional to the fraction of crystallized ferromagnetic phase. By the isothermal measurement of I_s around the crystallization temperature, the kinetics of crystallization can be analyzed. In Fig. 4, ln[1/(1 – X)] (where X is fraction transformed) was logarithmically plotted against time, according to the Johnson-Mehl-Avrami kinetic law.[21-24] This plot falls in straight lines and the slope n is almost independent of temperature, as shown in Fig. 4. This means that the precipitation of αFe proceeds by the usual nucleation and growth process.

3.3 *Soft Magnetic Properties and Their Thermal Stability*

As an example of soft magnetic properties of carbide-dispersed Fe-M-C films, Fig. 5 shows the frequency characteristics of relative permeability |μ| of $Fe_{78.6}Ta_{10.5}C_{10.9}$ films. These films exhibit high permeability, more than 5000 at 1 MHz, when they are annealed in static or rotating magnetic field. However, sufficiently high permeability of 2000 to 3000 is also obtained by annealing without a magnetic field. The

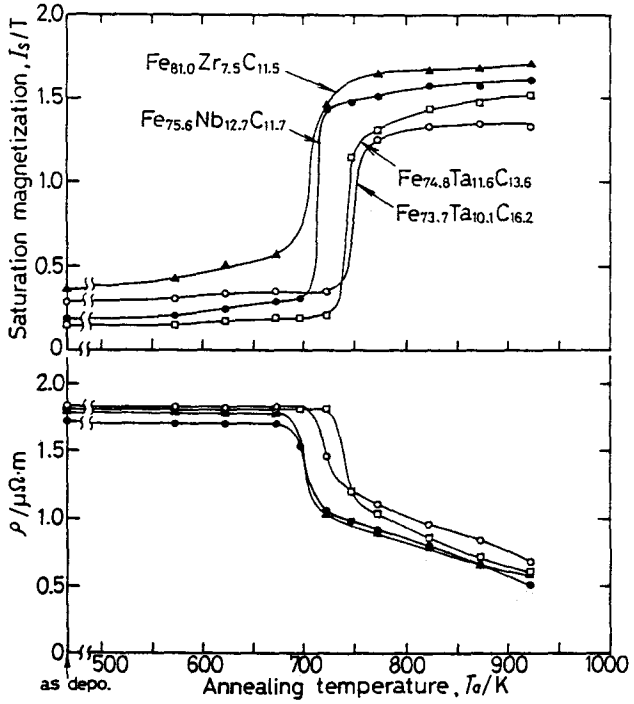

Fig. 3 Annealing temperature dependence of saturation magnetization, I_s, and resistivity, ρ, measured at room temperature. Annealing time at each temperature, 1.2 ks.

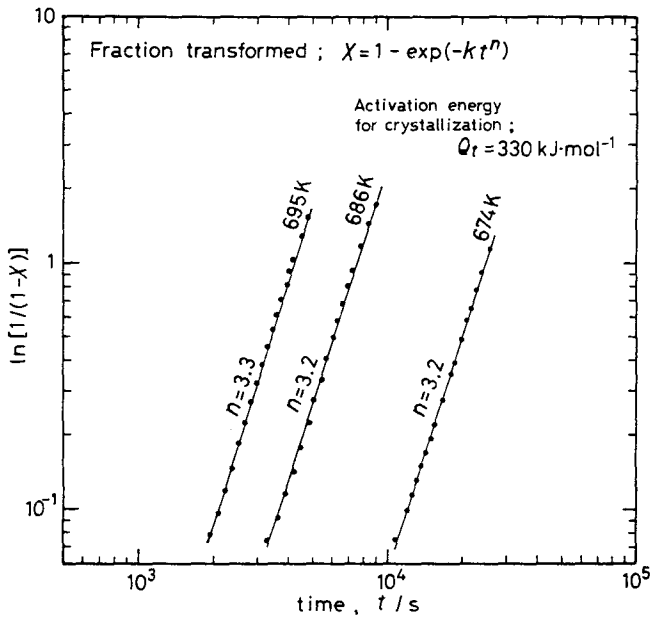

Fig. 4 Johnson-Mehl-Avrami plots of crystallization of ferromagnetic phases in $Fe_{81.4}Ta_{8.3}C_{10.3}$ films. Activation energy, Qt, was obtained by an Arrhenius plot of the time to 50% crystallization.

Table 1 Saturation magnetization, I_s, coercivity, Hc, relative permeability, |μ|, at 1 MHz, and magnetostriction, λs, of typical Fe-M-C films annealed at 823 K for 1.2 ks in a static magnetic field

M group	Film composition	I_s, T	Hc (a), A/m	|μ| (a) at 1 MHz	λs, 10^{-6}
IVA	$Fe_{75.7}Ti_{9.7}C_{14.6}$	1.71	354	670	+0.4
	$Fe_{84.3}Zr_{5.2}C_{10.5}$	1.72	20	6500	+1.2
	$Fe_{83.5}Hf_{5.9}C_{10.6}$	1.72	6	4310	+1.4
VA	$Fe_{70.3}V_{14.7}C_{15.0}$	1.64	188	770	–0.7
	$Fe_{73.5}Nb_{13.1}C_{13.4}$	1.48	7	4870	+0.1
	$Fe_{81.4}Ta_{9.7}C_{8.9}$	1.54	8	5250	–0.4

Note: Film thickness, 5 μm. (a) Along hard axis.

uniaxial anisotropy induced by static field annealing of this film is 100 to 200 A/m in anisotropy field *Hk*, which appears suitable for obtaining high permeability in the hard axis. On the other hand, Co-M-C films exhibit large induced uniaxial anisotropy of 1.6 kA/m in *Hk* after static field annealing. Therefore, the reduction of *Hk* by rotating field annealing or other heat treatment is necessary to obtain high permeability in Co-M-C films. In Table 2, magnetic properties of typical Co-M-C films (M = group IVa-VIa) annealed at 823 K in a rotating field are summarized. Of these films, Co-Cr-C films do not become soft magnetic, probably because Cr has great solubility in Co and less carbide-forming tendency compared to the group IVa or Va elements, resulting in relatively coarse grains.

By comparing Table 1 and Table 2, it can be observed that *Hc* of Co-M-C films is five to ten times as large as that of Fe-M-C films, notwithstanding their smaller grain size than in Fe-M-C films. This is probably due to the large intrinsic magnetocrystalline anisotropy of Co, which is an order of magnitude larger than that of Fe.

Ni-M-C films did not become soft magnetic after nanocrystallization in the present experiment. This is probably due to the presence of an anisotropy component perpendicular to the film plane induced by the combination of their large negative magnetostriction ($\lambda s < -10^{-5}$) and isotropic tensile stress ($<10^8$ Pa) in the film plane. The perpendicular anisotropy component is easily induced due to their small saturation magnetization (small demagnetization field perpendicular to the film plane).

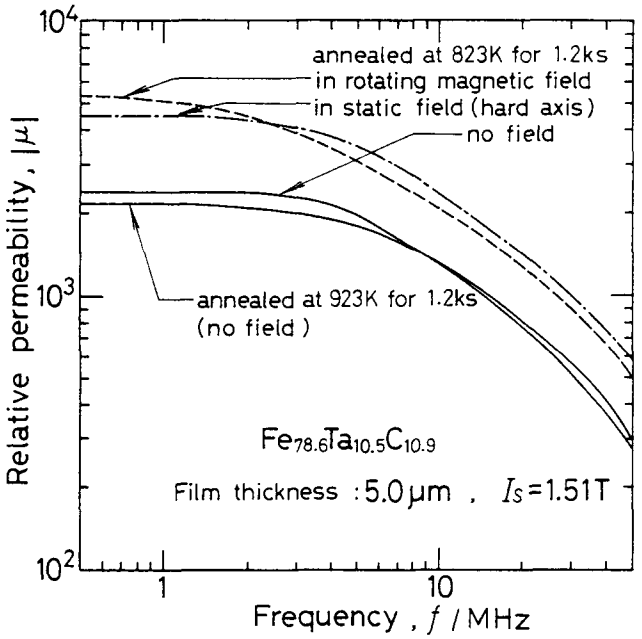

Fig. 5 Frequency characteristics of relative permeability |μ| for $Fe_{78.6}Ta_{10.5}C_{10.9}$ films that were 5 μm thick.

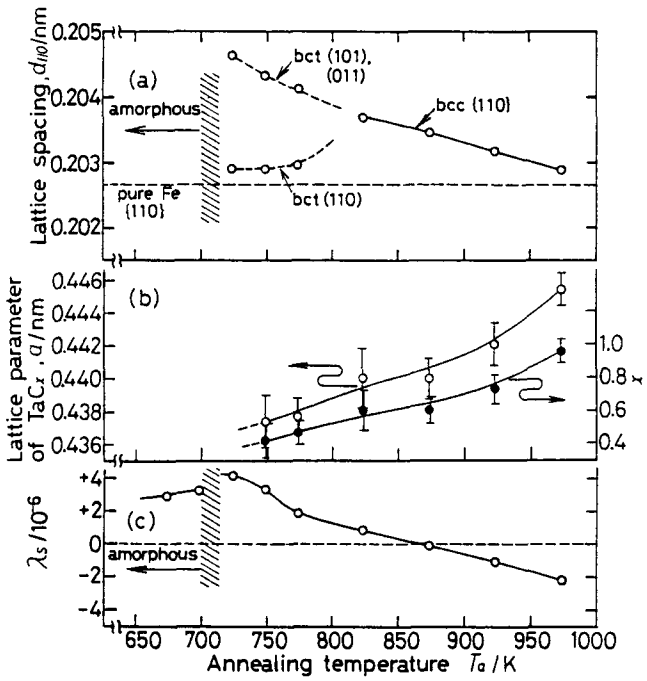

Fig. 6 Annealing temperature dependence of {110} lattice spacing of Fe d_{110} (a), lattice parameter *a* and composition *x* (estimated from *a*) of TaC_x (b), and magnetostriction λs (c) for $Fe_{81.4}Ta_{8.3}C_{10.3}$ films. Annealing time at each temperature, 1.2 ks.

Table 2 Saturation magnetization, I_s, coercivity, *Hc*, relative permeability, |μ|, at 1 MHz, and magnetostriction, λs, of typical Co-M-C films annealed at 823 K for 1.2 ks in a rotating magnetic field

M group	Film composition	I_s, T	*Hc*, A/m	|μ| (a) at 1 MHz	λs, 10^{-6}
IVa	$Co_{79.9}Ti_{10.6}C_{9.5}$	1.48	50	2240	−2.7
	$Co_{77.6}Zr_{10.8}C_{11.6}$	1.27	43	1530	−4.6
	$Co_{89.8}Zr_{3.5}C_{6.7}$	1.62	197	1770	−2.6
	$Co_{78.0}Hf_{10.9}C_{11.1}$	1.33	29	1900	−6.1
	$Co_{88.6}Hf_{2.8}C_{8.6}$	1.63	50	2440	−3.5
Va	$Co_{78.7}V_{9.9}C_{11.4}$	1.50	186	1280	−2.3
	$Co_{79.3}Nb_{10.0}C_{10.7}$	1.43	79	1930	−3.4
	$Co_{79.5}Ta_{9.8}C_{10.7}$	1.33	46	1720	−3.3
VIa	$Co_{72.4}Cr_{12.3}C_{15.3}$	0.84	>3000	<10	...
	$Co_{75.4}Mo_{11.1}C_{13.5}$	1.30	43	2320	−3.8
	$Co_{75.2}W_{10.5}C_{14.3}$	1.05	560	220	−3.2

Note: Film thickness, 5 μm. (a) Along hard axis.

As mentioned above, the Fe lattice in nanocrystalline Fe-M-C films is slightly expanded compared to the pure Fe lattice. It is important to analyze the relation between the structure and magnetic properties as a function of annealing temperature. In Fig. 6, annealing temperature dependence of {110} lattice spacing of Fe crystallites (a), lattice parameter a, and composition x (estimated from a) of TaC_x (b), and magnetostriction λs (c) for $Fe_{81.4}Ta_{8.3}C_{10.3}$ film is shown. The {110} diffraction peak of Fe after annealing at relatively low temperatures is split into two. This peak splitting becomes indistinct as the annealing temperature increases and the lattice spacing approaches that of pure Fe. This suggests that the Fe crystallite right after crystallization is a supersaturated solid solution of C with a tetragonally deformed lattice like martensite, and this gradually changes to the bcc Fe. The dissolution of a considerable amount of C in an Fe grain recently was directly detected by atom probe analysis.[19] This analysis also indicated the possibility of a small amount of Ta dissolution in Fe grains. This may stabilize the martensite-like structure, which decomposes below 700 K in conventionally quenched Fe-C alloys. Generally, C atoms interstitially dissolved into an Fe lattice usually cause a magnetic aftereffect, resulting in an instability of permeability. However, the magnetic aftereffect in the nanocrystalline Fe-Ta-C films was found to be suppressed considerably compared to quenched bulk Fe-C alloys (supersaturated bcc Fe-C solid solution).[25] This may be due to the presence of Ta, which can trap C atoms and decrease their mobility. On the other hand, the rejected C from Fe grains on higher temperature annealing is taken into TaC_x, and the lattice spacing of TaC_x gradually increases, as shown in Fig. 6(b). Along with the structural change in the Fe crystallite, λs changes its sign from positive to negative as annealing temperature increases and passes the zero line at around 873 K. This temperature becomes higher as the C to M ratio of the film increases. It appears that λs is correlated with the concentration of C in the Fe grains. That observation is consistent with the report on sputtered Fe-C films[26] with supersaturated C dissolved in an Fe lattice, whose λs also

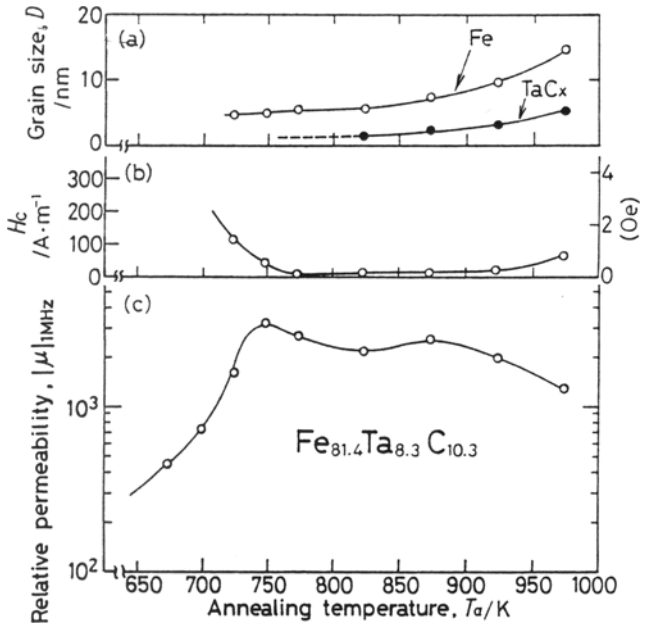

Fig. 7 Annealing temperature dependence of grain size, D (a), coercivity, Hc (b), and relative permeability $|\mu|$ at 1 MHz (c) for $Fe_{81.4}Ta_{8.3}C_{10.3}$ films that were 5 μm thick. Annealing time at each temperature, 1.2 ks.

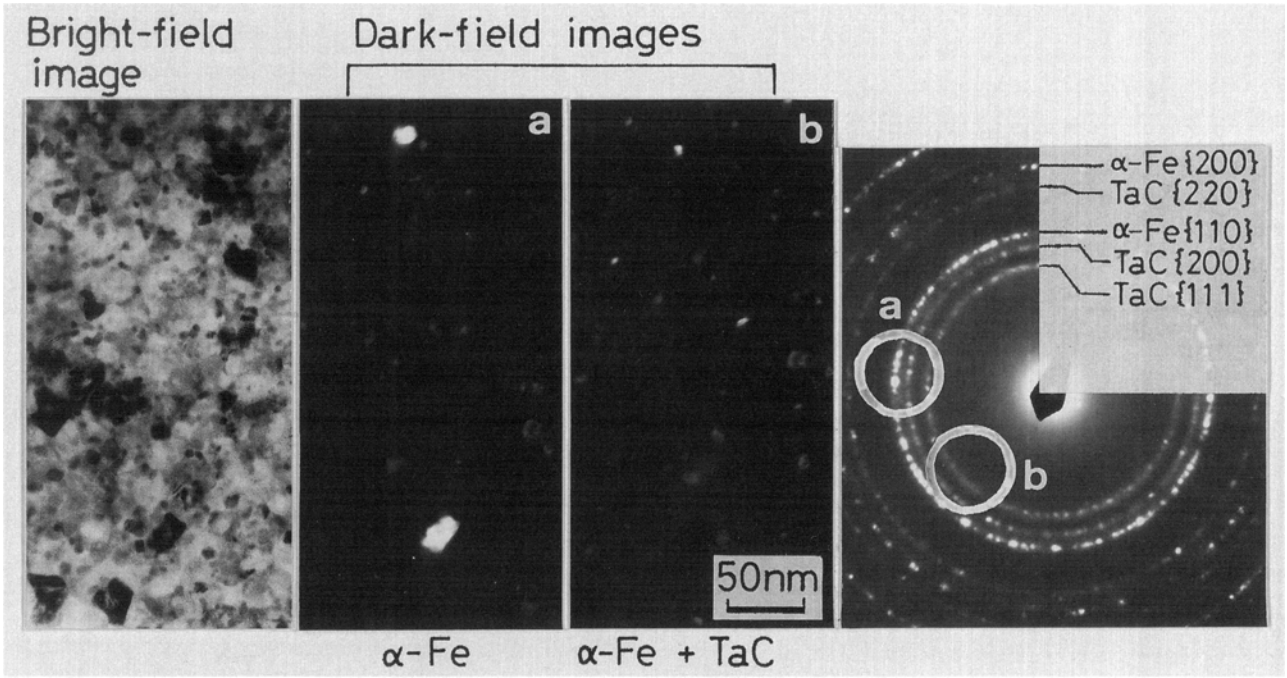

Fig. 8 TEM images and electron diffraction pattern of $Fe_{81.4}Ta_{8.3}C_{10.3}$ film annealed at 973 K for 1.2 ks. The dark-field images (a and b) were taken with an objective aperture indicated with the circles in the diffraction pattern.

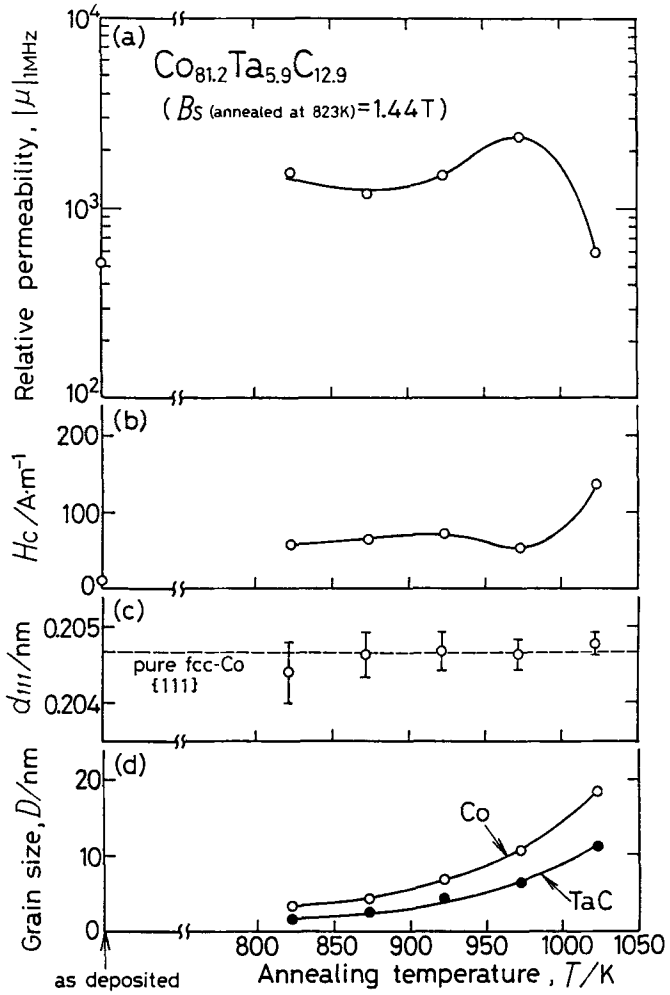

Fig. 9 Annealing temperature dependence of relative permeability |μ| at 1 MHz (a), coercivity, *Hc* (b), {111} lattice spacing of fcc Co d_{111} (c), and grain size, *D* (d) for $Co_{81.2}Ta_{5.9}C_{12.9}$ films that were 5 μm thick. Annealing was performed in a rotating magnetic field. Annealing time at each temperature, 1.2 ks.

changes from positive to negative as C concentration decreases.

Figure 7 shows the annealing temperature dependence of Fe and TaC_x grain size calculated from the half maximum breadth of X-ray diffraction peaks using Scherrer's equation (a), coercivity *Hc* (b), and relative permeability |μ| at 1 MHz (c) for the same film shown in Fig. 6. By comparing the curves of *Hc* and |μ| with that in λ*s* already shown in Fig. 6, λ*s* appears to have no significant influence on *Hc* or μ. Instead, μ and *Hc* in Fig. 7 appear to be influenced by grain size. This suggests that maintaining the nanocrystalline structure is more important for these films than controlling magnetostriction. As shown in Fig. 7(a), grain growth in this film is sluggish. As a result, this film exhibited $|\mu|_{1\,MHz}$ = 1300 and *Hc* = 65 A/m even after annealing at 973 K for 1.2 ks. Such high thermal stability of soft magnetic properties is due to the suppression of the Fe grain growth by pinning their grain boundaries by finely dispersed carbides. Figure 8 shows the TEM images and electron diffraction pattern of the $Fe_{81.4}Ta_{8.3}C_{10.3}$ film annealed at 973 K for 1.2 ks. As shown in the dark-field image of TaC (Fig. 8b), the TaC grain size grew larger and the number of TaC grains became fewer than in the film annealed at 823 K (Fig. 1A). This suggests that the growth of TaC proceeds by Ostwald ripening[27-29] driven by the diffusion through Fe grains or grain boundaries. Because the grain size of the primary phase is proportional to that of the dispersed particles, as theoretically predicted,[30] the stability of the nanocrystalline structure is expected to be higher in the film containing the carbides with a lower growth rate due to the smaller diffusion coefficient (higher melting point). In Table 3, the upper limit of annealing temperatures (annealing time, 1.2 ks) up to which *Hc* is less than 200 A/m is given for Fe-M-C films/M = 11 to 13 at.%, C = 10 to 14 at.%) containing various M-carbides, compared with the crystallization temperatures, *Tx*, measured by DSC (heating rate, 0.167 K/s) and melting points of M-carbides. This table shows that the upper limit of the annealing temperature is correlated to *Tx*, as well as to the melting point. Of these elements M, Hf, and Ta with a high melting point and *Tx* is the best for obtaining high thermal stability.

Table 3 Crystallization temperature, *Tx*, measured by DSC, upper limit of annealing temperature, *T (annealing time, 1.2 ks), up to which *Hc* less than 200 A/m is maintained, and melting point of M-carbides for Fe-M-C films (M = 11 to 13 at.%, C = 10 to 14 at.%)**

Film composition	*Tx*, K	Upper limit of annealing temperature, K	Melting point of carbide, K
$Fe_{76.3}Ti_{13.8}C_{9.9}$	665	720	3413 (TiC)
$Fe_{77.0}Zr_{13.2}C_{9.8}$	741	960	3803 (ZrC)
$Fe_{73.9}Hf_{12.1}C_{14.0}$	750	~1030	4160 (HfC)
$Fe_{73.1}V_{12.9}C_{14.0}$ (a) ...	705	...	3103 (VC)
$Fe_{76.8}Nb_{11.6}C_{11.6}$	736	940	3779 (NbC)
$Fe_{78.6}Ta_{10.5}C_{10.9}$	765	~1000	4150 (TaC)

(a) As-deposited film contains crystalline phase.

In nanocrystalline Fe-Cu-Nb-Si-B alloys,[4] a Nb- and B-enriched amorphous phase remaining at the grain boundaries was observed.[10,17] This intergranular amorphous phase is believed to retard the growth of Fe-Si nanocrystallites in these alloys. On the other hand, a residual amorphous phase like that observed in Fe-Cu-Nb-Si-B alloy by magnetic measurement[10] or by HRTEM[17] was not observed in Fe-Ta-C films using both these methods.[14] In the Fe-Cu-Nb-Si-B alloys, rapid grain growth and precipitation of Fe borides occurred along with the crystallization of the residual amorphous phase around 900 K. In Fe-M-C films, however, neither significant phase decomposition nor rapid grain growth takes place even on annealing at 973 K, as shown in Fig. 8, because the substance stabilizing the Fe(-C) nanocrystallites in Fe-M-C films is an M-carbide crystallite that is much more stable than the amorphous phase.

Figure 9 shows the annealing temperature dependence of |μ| at 1 MHz (a), *Hc* (b), {111} lattice spacing of fcc Co (c), and grain size calculated from the width of the X-ray diffraction peak for $Co_{81.2}Ta_{5.9}C_{12.9}$ film. Annealing was performed in a rotating magnetic field. The good soft magnetic properties of the Co-Ta-C film were also maintained even after annealing at

973 K, due to the suppression of grain growth by TaC. In Co-Ta-C films, the lattice spacing of Co is close to that of pure Co, regardless of annealing temperature, unlike the Fe-Ta-C films mentioned above. Therefore, a significant relationship between λs and annealing temperature or film composition was not found in Co-M-C films. Most of the Co-M-C films exhibited a negative λs, as shown in Table 2. Although it is difficult to obtain zero-magnetostrictive Co-M-C films by controlling annealing conditions or the C to M ratio, zero-magnetostriction was achieved by the addition of Fe, Ni, Mn, or Pd, which dissolves into Co and stabilizes the fcc phase.[13]

3.4 *Composition Dependence of Magnetic Properties*

In Fig. 10, the composition dependence of *Hc* for Fe-Ta-C films after annealing at 823 K for 1.2 ks is shown. The zero-magnetostrictive line is also shown in this figure. This zero-λs line shifts toward the C-rich side as the annealing temperature increases. This shift is related to a decrease in the amount of solute C in Fe grains, as mentioned above. This shift in the zero-λs line, however, does not accompany the shift in the minimum *Hc* region.[12] This suggests that the effect of λs on soft magnetic properties is obscured by other effects, which are considered to be caused primarily by microstructure. In this alloy system, films with high concentration of both Ta and C (Ta > 14 at.% and C > 14 at.%) do not become soft magnetic notwithstanding their fine grain structure. In these films, too many TaC particles precipitated at the grain boundaries may interrupt the intergranular exchange interaction, which plays an important role in their soft magnetism. In addition, it is also noted from Fig. 10 that the films with a concentration of C much higher than Ta or with a concentration of Ta higher than C also have poor soft magnetic properties. It was found by TEM observation that the excessively C-rich nanocrystalline films contain Fe_3C and a small amount of abnormally grown grains. Soft magnetic properties in these films are deteriorated probably due to the presence of the Fe_3C with an order of magnitude larger magnetocrystalline anisotropy than that of Fe[31] and to the structural inhomogeneity. On the other hand, the poor soft magnetic properties of the Ta-rich films is explained in terms of interruption of intergranular exchange coupling by the almost nonmagnetic residual amorphous phase, which was detected by the measurement of temperature dependence of *Hc*.[32]

As also shown in Fig. 10, the maximum Fe concentration of the films that exhibit low *Hc* values after annealing is limited primarily by the amorphization limit in the as-deposited state; this limit is shown as a shaded band in the figure. Although the grains of the films with Fe concentrations higher than this limit are small in the as-deposited state, they grow larger, probably before M-carbides precipitate. It was revealed by TEM observation that the film with a mixed amorphous and crystalline phase in the as-deposited state becomes inhomogeneous in grain size by annealing. The uniform and fine grain structure with finely dispersed M-carbides is obtained only when films are crystallized from the amorphous state. Therefore, it would be effective to use other M elements with higher amorphous forming ability to achieve higher saturation magnetization, I_s. For other Fe-M-C films containing 11 to 17 at.% C, the M concentration range over which an amorphous phase forms in an as-deposited state is shown in Fig. 11, as compared with that for Fe-Ta-C films. As can be seen in this figure, Zr and Hf have higher amorphous forming ability than Ta. As an example, Fig. 12 shows the composition dependence of *Hc* and I_s for Fe-Hf-C films after annealing at 823 K for 1.2 ks. In this system, the band of amorphization limit in the as-deposited state lies in an Fe-richer region than in the Fe-Ta-C system. As a result, the highest I_s of 1.7 T is obtained for soft magnetic Fe-Hf-C films, although the maximum I_s for Fe-Ta-C films is 1.6 T. In the same manner, I_s of 1.7 T is also achieved in Fe-Zr-C films. Because Hf and Ta contribute to good thermal stability, among those elements M, Hf is the preferred choice to simultaneously achieve high I_s and high thermal stability.

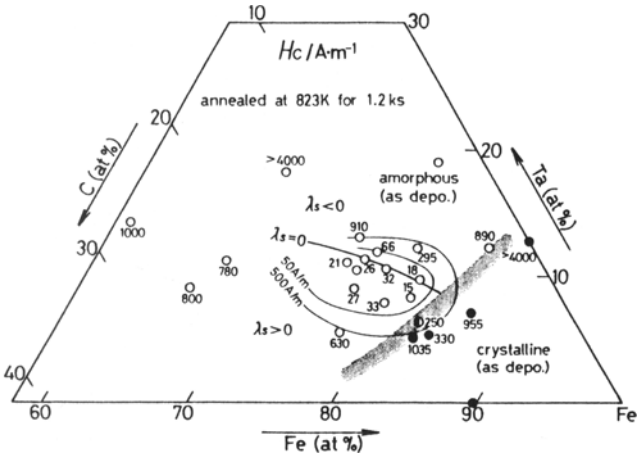

Fig. 10 Composition dependence of coercivity, *Hc*, for Fe-Ta-C films annealed at 823 K for 1.2 ks.

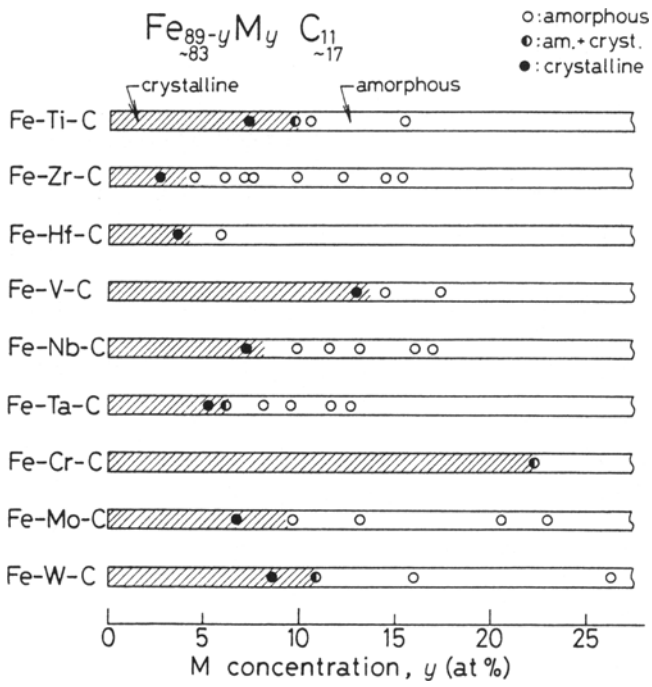

Fig. 11 M concentration range over which amorphous phases form in as-deposited films containing 11 to 17 at.% C.

In Fig. 13, composition dependence of Hc and I_s for Co-Ta-C films after annealing at 823 K in a rotating field is shown. The composition range over which good soft magnetic properties are obtainable is wider than in the Fe-Ta-C system, probably because the residual amorphous phase in Ta-rich films has a higher Curie temperature and is more soft magnetic than that in the Ta-rich Fe-Ta-C films. The maximum I_s obtained for Co-Ta-C films is 1.5 T. A higher value of I_s, 1.6 T, was obtained in Co-Zr-C and Co-Hf-C films, as shown in Table 2.

3.5 *Further Improvement of Performance of Carbide-Dispersed Nanocrystalline Films*

3.5.1 *Fe-Co-Hf-C Films with Higher I_s*

Further high I_s values are achieved by combining Fe and Co. With Co additions of less than 10 at.% to Fe-M-C films, I_s can be increased by several percent without any significant increase in anisotropy field or magnetostriction. For example, $Fe_{72.5}Co_{8.6}Hf_{5.0}C_{13.9}$ films exhibited I_s of 1.86 T and $|\mu|_{1MHz}$ (hard axis) of 1680, and Hc (hard axis) of 60 A/m after annealing at 823 K for 1.2 ks in a static magnetic field. However, around the composition of Fe:Co = 6:4 where I_s reaches a maximum, only poor soft magnetic properties were obtained.[15]

3.5.2 *Fe/Fe-Hf-C Multilayers as 2 T Soft Magnets*[33]

By multilayering the Fe-Hf-C alloys with Fe, the grains in the Fe layer become comparably small to its layer thickness, because the growth of large columnar grains of Fe is interrupted by the amorphous Fe-Hf-C layers. A schematic cross-sectional view of the as-deposited multilayer is shown in Fig. 14(a). By annealing this multilayer, the Fe-Hf-C layer nanocrystallizes. Figure 15 shows the cross-sectional TEM image and electron diffraction pattern of Fe (21 nm) /$Fe_{83.5}Hf_{5.9}C_{10.6}$ (21 nm) multilayer annealed at 823 K for 1.2 ks. This structure is schematically shown in Fig. 14(b). The

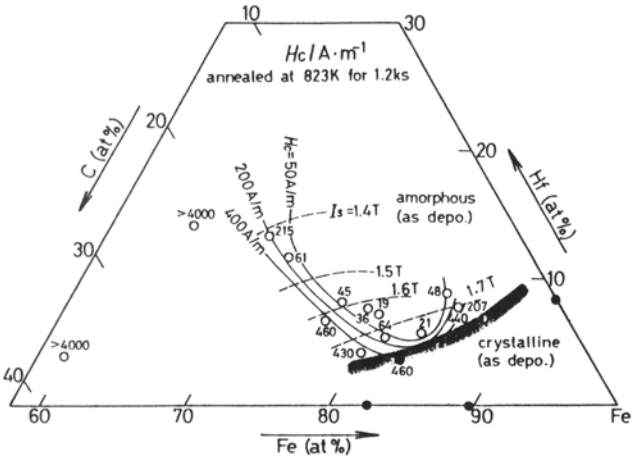

Fig. 12 Composition dependence of coercivity, Hc, and saturation magnetization, I_s, for Fe-Hf-C films annealed at 823 K for 1.2 ks.

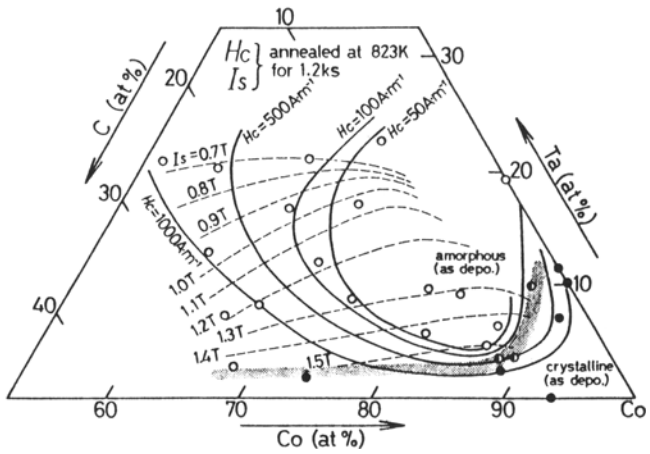

Fig. 13 Composition dependence of coercivity, Hc, and saturation magnetization, I_s, for Co-Ta-C films annealed at 823 K for 1.2 ks in rotating magnetic field.

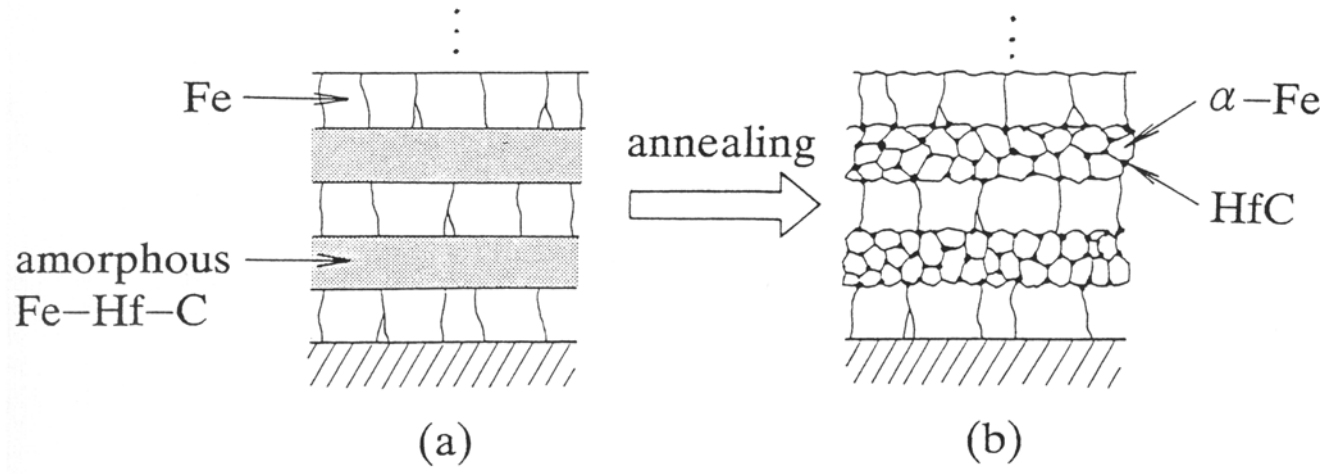

Fig. 14 Schematic of cross section of Fe/Fe-Hf-C multilayers.

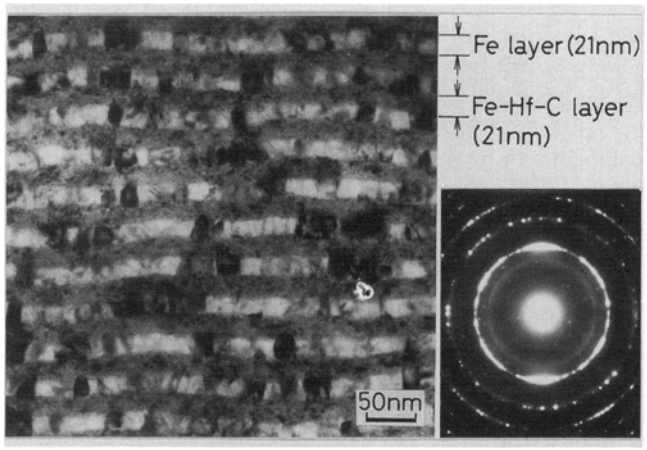

Fig. 15 Cross-sectional TEM image and electron diffraction pattern of Fe (21 nm)/$Fe_{83.5}Hf_{5.9}C_{10.6}$ (21 nm) multilayer annealed at 823 K for 1.2 ks.

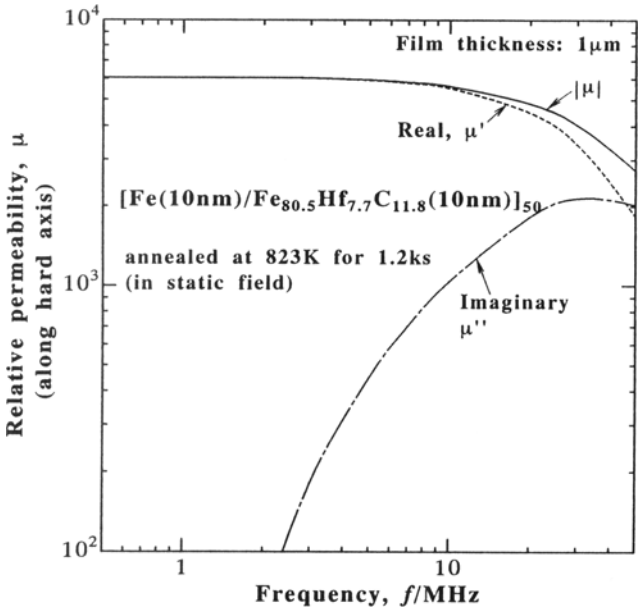

Fig. 16 Frequency characteristics of complex permeability along hard axis of [Fe(10 nm)/$Fe_{80.5}Hf_{7.7}C_{11.8}$ (10 nm)]$_{50}$ film annealed at 823 K for 1.2 ks in static magnetic field.

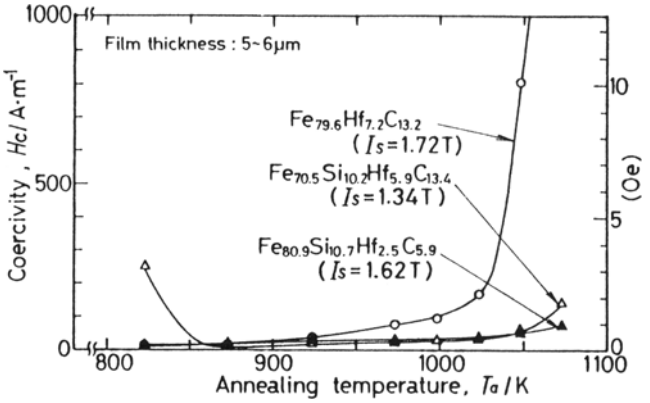

Fig. 17 Annealing temperature dependence of coercivity, *Hc*, for Fe-Hf-C and Fe-Si-Hf-C films. Annealing time at each temperature, 1.2 ks.

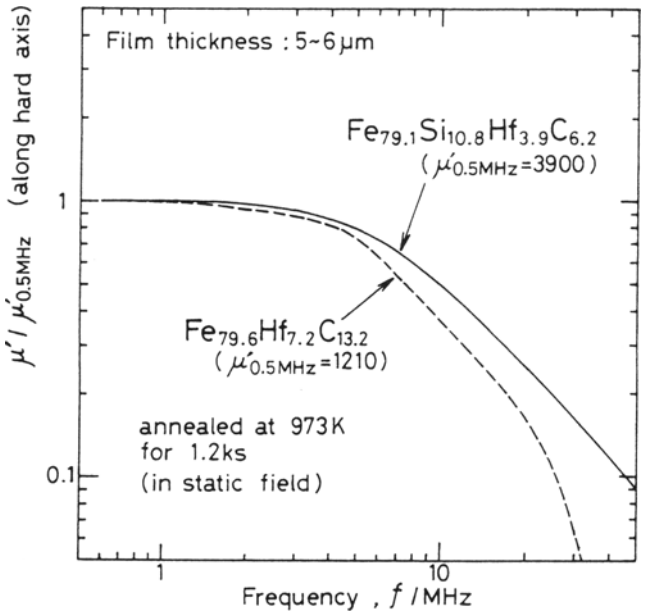

Fig. 18 Frequency characteristics of relative permeability, μ′ (real part, along hard axis) normalized by the μ′ at 0.5 MHz, for $Fe_{79.1}Si_{10.8}Hf_{3.9}C_{6.2}$ films compared to $Fe_{79.6}Hf_{7.2}C_{13.2}$ film annealed at 973 K for 1.2 ks in a static magnetic field. Film thickness, 5 to 6 μm.

grains in the Fe layer remain small compared to its layer thickness. Such nanocrystalline layered structure is maintained even on annealing around 1000 K, probably because the grain boundaries of the Fe layer are also pinned by the HfC precipitated at the interface between the Fe and Fe-Hf-C layers.[34] These multilayers simultaneously exhibit much higher I_s of 2.0 T than the single layer and thermal stability of their soft magnetic properties as high as single-layer Fe-Hf-C films. Figure 16 shows the frequency characteristics of complex permeability along hard axis of [Fe(10 nm)/$Fe_{80.5}Hf_{7.7}C_{11.8}$ (10 nm)]$_{50}$ films (film thickness, 1 μm) annealed at 823 K for 1.2 ks in a static magnetic field. As shown in this figure, the high permeability of 6000 is obtained in this high I_s film.

3.5.3 *Fe-Si-Hf-C Films with Higher Thermal Stability and Permeability at High Frequency*[35]

Amorphous Fe-Si-Hf-C films also crystallize into nanocrystallites composed of Fe-Si solid solution and HfC particles. Because the Si contributes to the amorphization on sputter deposition, the Hf and C concentrations needed for amorphization decrease by the Si addition. Hence, the sufficiently high I_s of 1.6 T can be maintained by decreasing the Hf and C concentration, even when 10 at.% Si is added. In Fig. 17, the annealing temperature dependence of coercivity *Hc* of films with and without Si is shown. As shown in this figure, the Fe-Si-Hf-C

films exhibit about 100 K higher thermal stability than the Fe-Hf-C film. This improvement appears to be attributed primarily to the further retardation of grain growth by the alloying effect, rather than the decrease in intrinsic magnetocrystalline anisotropy by Si dissolution into Fe.

In addition to the improvement of thermal stability, the frequency characteristics of relatively thick films are also improved by the Si addition. Figure 18 shows the frequency characteristics of relative permeability μ' (real part) normalized by the μ' at 0.5 MHz for the 5 to 6 μm thick films. This improvement in high-frequency permeability is considered to be primarily due to the suppression of eddy current losses, because Si additions raise the film resistivity by three to five times.

4. Conclusions

Nanocrystalline Fe-M-C, Co-M-C, and Ni-M-C (M = Zr, Hf, Nb, Ta, etc.) films in which extremely fine M-carbide particles are dispersed were prepared by annealing sputter-deposited amorphous alloy films. Of these films, Fe-M-C and Co-M-C films exhibit good soft magnetic properties. The dispersed carbide particles in these films considerably retard the grain growth of Fe- or Co-rich nanocrystallite by pinning their grain boundaries. This results in high thermal stability of their soft magnetic properties due to the nanocrystalline structure. The nanocrystalline Fe-M-C films exhibit higher saturation magnetization I_s and better soft magnetic properties than the Co-M-C films. Moreover, zero-magnetostrictive Fe-M-C films can easily be attained by controlling the C to M ratio or annealing conditions. Among M (group IVa-VIa) elements, Ta and Hf are suitable for thermal stability, and Zr and Hf are suitable for obtaining high I_s of 1.7 T. Therefore, Hf is the best element for improving both properties.

By multilayering Fe-Hf-C films with Fe, further increases in I_s are possible up to 2.0 T. This is achieved without sacrificing the soft magnetic properties or thermal stability. Alternatively, thermal stability and permeability in the high-frequency region of Fe-Hf-C films is further improved by addition of Si without significant decrease in I_s. Those carbide-dispersed nanocrystalline films are suitable for use in high-density magnetic recording heads fabricated by the glass bonding process (e.g., metal-in-gap type heads or sandwich-type heads).

References

1. N. Kumasaka, N. Saito, Y. Shiroishi, K. Shiiki, H. Fujiwara, and M. Kudo, Magnetic Properties of Multilayered Fe-Si Films, *J. Appl. Phys.*, Vol 55(No. 6), 1984, p 2238-2240
2. T. Kobayashi, R. Nakatani, S. Ootomo, and N. Kumasaka, Magnetic Properties of Multilayered Fe-C Films Formed by Dual Ion Beam Sputtering, *IEEE Trans. Magn.*, Vol MAG-23(No. 5), 1987, p 2746-2748
3. F.W.A. Dirne, F.J.A. den Broeder, J.A.M. Tolboom, H.J. de Wit, and C.H.M. Witmer, Soft-Magnetic Properties and Structure of Fe/Co-Nb-Zr Multilayers, *Appl. Phys. Lett.*, Vol 53(No. 24), 1988, p 2386-2388
4. Y. Yoshizawa, S. Oguma, and K. Yamauchi, New Fe-Based Soft Magnetic Alloys Composed of Ultrafine Grain Structure, *J. Appl. Phys.*, Vol 64(No. 10), 1988, p 6044-6046
5. M. Senda and Y. Nagai, Magnetic Properties of Fe/SiO_2 Multilayer Film, *J. Appl. Phys.*, Vol 65(No. 3), 1989, p 1238-1242
6. H. Sakakima, K. Ihara, K. Osano, and N. Kaminaka, Magnetic Properties of Compositionally Modulated Fe-Based Nitride Alloy Films, *IEEE Trans. Magn.*, Vol 26(No. 5), 1990, p 2347-2349
7. F.W.A. Dirne and M. Brouha, Soft-Magnetic Properties of Microcrystalline Co-Fe-Si-B Alloys Prepared by Sputtering, *IEEE Trans. Magn.*, Vol 24(No. 2), 1988, p 1862-1864
8. H. Hoffmann, Quantitative Calculation of the Magnetic Ripple of Uniaxial Thin Permalloy Films, *J. Appl. Phys.*, Vol 35(No. 6), 1964, p 1790-1798
9. M. Takahashi and T. Shimatsu, Soft Magnetism of Crystalline Fe-Based Alloy Sputtered Films, *IEEE Trans. Magn.*, Vol 26(No. 5), 1990, p 1485-1490
10. G. Herzer, Grain Size Dependence of Coercivity and Permeability in Nanocrystalline Ferromagnets, *IEEE Trans. Magn.*, Vol 26(No. 5), 1990, p 1397-1402
11. N. Hasegawa and M. Saito, "Soft Magnetic Properties of Microcrystalline Fe-M-C (M = Ti,Zr,Hf) Films with High Thermal Stability (in Japanese)," IEICE Technical Report, MR89-12, 1989
12. N. Hasegawa and M. Saito, Soft Magnetic Properties of Microcrystalline Fe-M-C (M = V,Nb,Ta) Films with High Thermal Stability, *IEEE Trans. J. Magn. Jpn.*, Vol 6(No. 1), 1991, p 91-100; originally published in *J. Magn. Soc. Jpn.*, Vol 14(No. 2), 1990, p 313-318
13. N. Hasegawa and M. Saito, Soft Magnetic Properties of Microcrystalline Co-M-C (M:group IVa-VIa elements) Films with High Thermal Stability (in Japanese), *J. Jpn. Inst. Met.*, Vol 54(No. 11), 1990, p 1270-1278
14. N. Hasegawa, N. Kataoka, K. Hiraga, and H. Fujimori, Microstructure of Carbide-Dispersed Nanocrystalline Fe-Ta-C Films, *Mater. Trans. JIM*, Vol 33(No. 6), 1992, p 632-635
15. N. Hasegawa and M. Saito, Structural and Soft Magnetic Properties of Nanocrystalline (Fe,Co,Ni)-Ta-C Films with High Thermal Stability, *J. Magn. Magn. Mater.*, Vol 103(No. 3), 1992, p 274-284
16. N. Kataoka, A. Inoue, T. Masumoto, Y. Yoshizawa, and K. Yamauchi, Effect of Additional Cu Element on Structure and Crystallization Behavior of Amorphous Fe-Nb-Si-B Alloys, *Jpn. J. Appl. Phys.*, Vol 28(No. 10), 1989 p L1820-L1823
17. K. Hono, K. Hiraga, Q. Wang, A. Inoue, and T. Sakurai, The Microstructure Evolution of a $Fe_{73.5}Si_{13.5}B_9Nb_3Cu_1$ Nanocrystalline Soft Magnetic Material, *Acta Metall. Mater.*, Vol 40(No. 9), 1992, p 2137-2147
18. N. Hasegawa, M. Saito, A. Kojima, A. Makino, Y. Misaki, and T. Watanabe, Crystallization Behavior of Fe-M-C (M = Ti, Zr, Hf, V, Nb, Ta) Films, *IEEE Trans. J. Magn. Jpn.*, Vol 6(No. 2), 1991, p 120-126; originally published in *J. Magn. Soc. Jpn.*, Vol 14(No. 2), 1990, p 319-322
19. K. Hono, N. Hasegawa, S.S. Babu, H. Fujimori, and T. Sakurai, Atom Probe Analysis of Nanocrystalline Fe-C-Ta Sputtered Soft Magnetic Thin Film, *Surf. Sci.*, in press
20. K.A. Taylor, L. Chang, G.B. Olson, G.D.W. Smith, M. Cohen, and J.B. Vander Sande, Spinodal Decomposition during Aging of Fe-Ni-C Martensites, *Metall. Trans. A*, Vol 20, 1989, p 2717-2737
21. W.A. Johnson and R.F. Mehl, Reaction Kinetics in Processes of Nucleation and Growth, *Trans. AIME*, Vol 135, 1939, p 416-458
22. M. Avrami, Kinetics of Phase Change. I. General Theory, *J. Chem. Phys.*, Vol 7, 1939, p 1103-1112
23. M. Avrami, Kinetics of Phase Change. II. Transformation-Time Relation for Random Distribution of Nuclei, *J. Chem. Phys.*, Vol 8, 1940, p 212-224
24. M. Avrami, Granulation, Phase Change, and Microstructure, Kinetics of Phase Change. III, *J. Chem. Phys.*, Vol 9, 1941, p 177-184

25. N. Hasegawa, H. Numakura, N. Kataoka, M. Koiwa, and H. Fujimori, "Magnetic Aftereffect and Induced Magnetic Anisotropy of Nanocrystalline Fe-Ta-C Films" (in Japanese), Digest of Fall Meeting of Jpn. Inst. Metals, 1992, p 327

26. T. Kobayashi, R. Nakatani, S. Ootomo, N. Kumasaka, and K. Shiiki, Soft Magnetic Properties of Fe-C/Ni-Fe Multilayered Films, *J. Appl. Phys.*, Vol 64(No. 6), 1988, p 3157-3162

27. G.W. Greenwood, The Growth of Dispersed Precipitates in Solutions, *Acta Metall.*, Vol 4, 1956, p 243-248

28. I.M. Lifshitz and V.V. Slyozov, The Kinetics of Precipitation from Supersaturated Solid Solutions, *J. Phys. Chem Solids*, Vol 19(No. 1/2), 1961, p 35-50

29. C. Wagner, Theorie der Alterung von Niederschlägen durch Umlösen (in German), *Z. Elektrochem.*, Vol 65(No. 7/8), 1961, p 581-591

30. C. Zener, cited by C.S. Smith, Grains, Phases, and Interfaces: An Interpretation of Microstructure, *Trans. AIME*, Vol 175, 1948, p 15-51

31. P. Blum and R. Pauthenet, Étude Ferromagnétique de la Cémentite Polycristalline et Monocristalline (in French), *CR Acad. Sci.*, Vol 237, 1953, p 1501-1502

32. N. Hasegawa, N. Kataoka, and H. Fujimori, "Nanocrystallization Behavior and Thermal Stability of Soft Magnetic Properties of Fe-Ta-C Alloy Films" (in Japanese), Digest of Fall Meeting of Jpn. Inst. Metals, 1991, p 246

33. N. Hasegawa, N. Kataoka, H. Fujimori, and M. Saito, Structural and Soft Magnetic Properties of Fe/Fe-Hf-C Multilayered Films with the High *Bs* and Thermal Stability, *J. Appl. Phys.*, Vol 70(No. 10), 1991, p 6253-6255

34. H. Fujimori, N. Hasegawa, N. Kataoka, S. Nagata, and S. Yamaguchi, Thermal Stability of Nanocrystalline Multilayered Structure in Soft Magnetic Fe/Fe-Hf-C Films, *J. Magn. Magn. Mater.*, in press

35. N. Hasegawa, N. Kataoka, and H. Fujimori, Soft Magnetic Properties of Carbide-Dispersed Nanocrystalline Fe-Si-Hf-C Films (in Japanese), *J. Magn. Soc. Jpn.*, Vol 16(No. 2), 1992, p 253-256